REGULARIZATION OF THE BOUNDARY INTEGRALS IN THE BEM ANALYSIS OF 3D POTENTIAL PROBLEMS

Y. C. Shiah *

Program of Mechanical and Aeronautical Engineering
Feng Chia University
Taichung, Taiwan 40724, R.O.C.

M. R. Hematiyan

Department of Mechanical Engineering
Shiraz University
Shiraz, Iran

Y. H. Chen

Department of Computer Science and Information Management
Providence University
Taichung, Taiwan 43301, R.O.C.

ABSTRACT

In the conventional boundary element analysis, near-singularities are present in the associated boundary integral equation for problems involving ultra-thin media. For this case, any conventional numerical schemes will fail to yield proper values for the integrals. In this paper, the boundary integrals of the boundary element method for 3D potential problems are fully regularized by the technique of integration by parts under the local coordinate system. The fully regularized integrands are expressed as very explicit formulations that can be easily programmed into a computer code. Numerical tests carried out for a typical case have verified the accuracy of the approach for any orders of small distance between the source and the element under integration.

Keywords: Boundary element method, Regularization of boundary integrals, 3D potential problems.

1. INTRODUCTION

Potential problems are present in engineering practice as an important topic that has been researched over the years. Although some typical problems (*e.g.* [1-3]) can be solved analytically by various techniques, it is quite often that solutions to complicated problems, especially in engineering practice, need resort to numerical tools. Up to this point regarding numerical methods for boundary-value problems, the most commonly applied techniques include the finite difference method (FDM), the finite element method (FEM), and the boundary element method (BEM). The FDM has an apparent advantage that the formulated finite-difference formulations are relatively simpler than those using the other techniques; however, extra efforts are required to take care of irregular boundary geometry. For acquiring accurate results by the FDM, the step size always plays a crucial role. At the expense of more elaborate formulations involved, the FEM, having been extensively applied in industries, is evidently advantageous over the FDM in handling complicated geometries. The FDM and the FEM are both characterized as domain-solution techniques that the entire domain needs discretization by "meshes" or "elements". For engineering problems, the BEM has been recognized as an efficient numerical tool due to its distinctive feature that only the boundary needs discretization in contrast with the domain-solution techniques. As a prelude of the BEM development, Rizzo [4], in 1967, presented a formulation of the so-called "direct method" for linear elasticity. Earlier than that, the so called "indirect method" was firstly presented by Lauricella in 1909 [5] and put forth by Massonnet [6] and Kupradze [7]. The direct and indirect method were examined and shown to be equivalent by Hong and Chen [8] in 1988.

In engineering analysis, it is quite often that the object of interest considers 3D heat conduction in a very thin or even ultra-thin media such as turbine blades, coating films, or bonding adhesives. For various purposes, the size-order of the thin media may be from the micro-scale to as low as the nano-scale. To yield reliable results for such problems, conventional modeling of the thin media by the FEM generally requires enormous amounts of elements due to the fact that the aspect ratios of modeling elements must not be smaller than 1/20. As an obvious consequence of this modeling limitation, the required vast number of elements may lead to overloading computation. Also, a similar modeling difficulty happens to the BEM too. The

* Corresponding author (ycshiah@fcu.edu.tw)

DOI : 10.1017/jmech.2012.140
Copyright © 2012 The Society of Theoretical and Applied Mechanics, R.O.C.
https://doi.org/10.1017/jmech.2012.140 Published online by Cambridge University Press

main cause of this difficulty in the BEM is directly derived from the nearly singular behaviors present in the boundary integrals for the 3D potential problems. Under the circumstance when the source is very close to the integration element, the fundamental solutions of the Green's function and its one-order derivatives are nearly strong-singular and nearly hyper-singular, respectively. The singular integrals are considered in the sense of Cauchy principal value (PV), while the hypersingular ones are considered the Hadamard finite part integrals (FP). Due to the rapid fluctuations of the integrands, any conventional numerical schemes shall fail to properly integrate them.

Over the years, this topic has attracted significant researches in the BEM community to overcome this difficulty. The most known approaches for treatment of the different divergent integrals can be referred to [9-12] for example. There are too many to review as a complete; only a few among them are mentioned herein as examples. Granados and Gallego [13] proposed a kernels' complex regularization procedure, leading to a decomposition of the quasi-singular and quasi-hypersingular integrals in a series of simpler terms. Recently, Tomioka and Nishiyama [14] presented a gradient field representation using an analytical regularization of a hypersingular boundary integral equation for the Helmholtz equation. For axisymmetric linear elasticity, de Lacerda and Wrobel [15] presented a hypersingular boundary integral equation, which are regularized by employing the singularity subtraction technique. On revisiting the same problem, On applying the technique of integration by parts, Shiah and Shi [16] regularized the boundary integrals for the 2D anisotropic heat conduction problems. Furthermore, Shiah *et al*. [17] applied this technique to study the interlaminar thermal stresses in thin layers of composites. It should be noted that, for singular function, the operation of integration by parts is not correct in classical sense; instead, it should be considered is the sense of distributions. Also, it is worth mentioning that a dual integral formulation for the Laplace problem with a smooth boundary was derived by Chen *et al.* [18] by using a contour approach surrounding the singularity. In their work, the definition for the Hadamard principal value for hypersingular integral at the collocation point of a smooth boundary was extended to a generalized sense. A more thorough review of the dual boundary element method with emphasis on the hypersingular integral can be found in Chen and Hong [10]. So far as we know, this technique of integration by parts has only been successfully applied to regularize the boundary integrals in the 2D BEM; however, no successful attempt has been reported to regularize the associated 3D cases, where two independent variables for the local coordinates are involved. This paper aims at applying this technique to regularize the boundary integrals for the associated 3D potential problems in the BEM. Very explicit formulations for the regularized integrals are presented that can be easily implemented in programming. For verifications, numerical tests are performed to show the accuracy of the reformulated integrals.

2. BOUNDARY INTEGRAL EQUATION FOR 3D POTENTIAL PROBLEMS

As has been well established in open literatures, potential problems without the presence of source terms are governed by the so called "Laplace equation", namely

$$\frac{\partial^2 \phi}{\partial x_1^2}+\frac{\partial^2 \phi}{\partial x_2^2}+\frac{\partial^2 \phi}{\partial x_3^2}=0\ , \tag{1}$$

where ϕ represents the potential. It is well known in the BEM literature that for a problem governed by the Laplace equation in three dimensions, the potential ϕ and its normal gradient $q = d\phi/dn$, where n is the unit outward normal, along the boundary of a solution domain are related by the following boundary integral equation,

$$c(P)\ \phi(P)=\int_S q(Q)U(P,\ Q)\,dS-\int_S \phi(Q)\,\frac{dU(P,\ Q)}{dn}\,dS\ , \tag{2}$$

where P and Q are the source and field points on the boundary, respectively; $c(P)$ is a constant depending on the geometry at P. In Eq. (2), the fundamental solutions $U(P, Q)$ and dU/dn are given by

$$U(P,\ Q)=\frac{1}{4\pi r}\ , \tag{3}$$

$$\frac{dU(P,\ Q)}{dn}=\frac{-n_i\ r_{,i}}{4\pi r^2}\ , \tag{4}$$

where n_i represent the components of the unit outward normal vector. Following the usual process in BEM analysis for solving Eq. (2), the solution boundary is discretized into an assemblage of quadrilateral and/or triangular elements, say M elements, each of which is defined by k nodes. Writing Eq. (2) for each of these distinct nodes and substituting into it appropriate shape functions $N^{(i)}$ for the interpolation of the solution variables will result in a set of simultaneous equations for the unknown potential or potential gradient at the nodes. For each of the j-th global node, one may have the discretized form of Eq. (2), expressed in the local coordinate system (ξ, η) as

$$c\,\phi_j=\sum_{m=1}^{M}\sum_{i=1}^{k}\frac{q_{(m)}^{(i)}}{4\pi}\int_{-1}^{1}\int_{-1}^{1}\frac{N^{(i)}J}{\sqrt{\sum_{l=1}^{3}\left(\sum_{c=1}^{k}N^{(c)}x_{l(m)}^{(c)}-xp_l\right)^2}}\,d\xi\,d\eta$$
$$-\sum_{m=1}^{M}\sum_{i=1}^{k}\frac{\phi_{(m)}^{(i)}}{4\pi}\int_{-1}^{1}\int_{-1}^{1}\frac{N^{(i)}\sum_{l=1}^{3}\left[(xp_l-\sum_{c=1}^{k}N^{(c)}x_{l(m)}^{(c)})J_l\right]}{\sqrt{\left[\sum_{l=1}^{3}(\sum_{c=1}^{k}N^{(c)}x_{l(m)}^{(c)}-xp_l)^2\right]^3}}\,d\xi\,d\eta\ , \tag{5}$$

where xp_l stands for the Cartesian coordinate of the source point; the subscript (m) and the super script (i) are used to denote the i-th node of the element m. In

https://doi.org/10.1017/jmech.2012.140 Published online by Cambridge University Press

Eq. (5), J and J_l, the Jacobian and its l-th component of the coordinate transformation for the element m, are given by

$$J_1 = \left(\sum_{c=1}^{k} N_{,\xi}^{(c)} x_{2(m)}^{(c)}\right)\left(\sum_{c=1}^{k} N_{,\eta}^{(c)} x_{3(m)}^{(c)}\right) - \left(\sum_{c=1}^{k} N_{,\xi}^{(c)} x_{3(m)}^{(c)}\right)\left(\sum_{c=1}^{k} N_{,\eta}^{(c)} x_{2(m)}^{(c)}\right), \quad (6a)$$

$$J_2 = \left(\sum_{c=1}^{k} N_{,\xi}^{(c)} x_{3(m)}^{(c)}\right)\left(\sum_{c=1}^{k} N_{,\eta}^{(c)} x_{1(m)}^{(c)}\right) - \left(\sum_{c=1}^{k} N_{,\xi}^{(c)} x_{1(m)}^{(c)}\right)\left(\sum_{c=1}^{k} N_{,\eta}^{(c)} x_{3(m)}^{(c)}\right), \quad (6b)$$

$$J_3 = \left(\sum_{c=1}^{k} N_{,\xi}^{(c)} x_{1(m)}^{(c)}\right)\left(\sum_{c=1}^{k} N_{,\eta}^{(c)} x_{2(m)}^{(c)}\right) - \left(\sum_{c=1}^{k} N_{,\xi}^{(c)} x_{2(m)}^{(c)}\right)\left(\sum_{c=1}^{k} N_{,\eta}^{(c)} x_{1(m)}^{(c)}\right), \quad (6c)$$

$$J = \sqrt{J_1^2 + J_2^2 + J_3^2}, \quad (6d)$$

where $N_{,\xi}^{(c)}$ and $N_{,\eta}^{(c)}$ denote taking differ entiation of the shape function with respect to ξ and η, respectively. As has been well developed, the shape functions for 8-node quadrilateral elements are given by

$$N^{(1)} = \frac{-1}{4}(1-\xi)(1-\eta)(1+\xi+\eta),\ N^{(2)} = \frac{1}{2}(1-\xi^2)(1-\eta),$$
$$N^{(3)} = \frac{1}{4}(1+\xi)(1-\eta)(\xi-\eta-1),\ N^{(4)} = \frac{1}{2}(1+\xi)(1-\eta^2),$$
$$N^{(5)} = \frac{1}{4}(1+\xi)(1+\eta)(\xi+\eta-1),\ N^{(6)} = \frac{1}{2}(1-\xi^2)(1+\eta),$$
$$N^{(7)} = \frac{1}{4}(1-\xi)(1+\eta)(-\xi+\eta-1),\ N^{(8)} = \frac{1}{2}(1-\xi)(1-\eta^2). \quad (7)$$

and, for 6-node triangular elements, they are

$$N^{(1)} = (1-\xi-\eta)(1-2\xi-2\eta),\quad N^{(2)} = 4\xi(1-\xi-\eta),$$
$$N^{(3)} = \xi(2\xi-1),\quad N^{(4)} = 4\xi\eta,$$
$$N^{(5)} = \eta(2\eta-1),\quad N^{(6)} = \frac{1}{2}(1-\xi^2)(1+\eta). \quad (8)$$

Since taking partial differentiation of the above shape functions can be readily performed, their partially differentiated forms are not explicitly given herein. On observing the integrands in Eq. (5), one may readily identify their quasi-singular and quasi-hypersingular natures for the first and the second integral, respectively, when the source point is very close to the element under integration. This nearly singular/hypersingular behavior leads to difficulty computing their numerical values properly due to the rapid fluctuations of these integrands at the projection coordinates (ξ_0, η_0) of the source point on the integration element. With reference to Fig. 1, the phenomenon is present when d, the distance between the source point and the project point, is much smaller than the characteristic dimension (D) of the element under integration. For brevity, the integrands in Eq. (5) are represented by

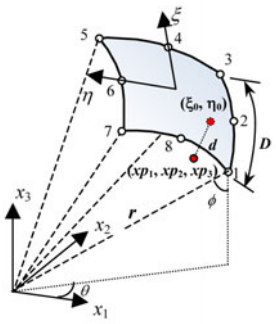


Fig. 1 Schematic representation of the source point and an integration element

$$G_i = \frac{N^{(i)} J}{\sqrt{\sum_{l=1}^{3}\left(\sum_{c=1}^{k} N^{(c)} x_{l(m)}^{(c)} - xp_l\right)^2}},$$
$$H_{is(m)} = \frac{\left(xp_s - \sum_{c=1}^{k} N^{(c)} x_{s(m)}^{(c)}\right) N^{(i)} J_s}{\sqrt{\left[\sum_{l=1}^{3}\left(\sum_{c=1}^{k} N^{(c)} x_{l(m)}^{(c)} - xp_l\right)^2\right]^3}}. \quad (9)$$

For simplifying formulations in later derivations, the subscript (m) denoting the element number is dropped from now on. Figures 2 and 3 show the respective fluctuations of the $G_i(\xi, \eta)$ and $\sum_{s=1}^{3} H_{is}(\xi, \eta)$ for a typical case of a quadrilateral element when the source point is projected onto $(\xi_0 = 0.5, \eta_0 = -0.3)$ with $d/D \approx 0.002$. As shown in these figures, spikes of the integrand values appear at the project point and, therefore, shall cause difficulties of proper numerical integrations. It is worth noting that, as revealed from the comparison between Figs. 2 and 3, $H_{is}(\xi, \eta)$ bears stronger singularity than that of $G_i(\xi, \eta)$, which will make its regularization more challenging. Next, the processes to regularize these nearly singular integrands, $G_i(\xi, \eta)$ and $H_{is}(\xi, \eta)$, will be elaborated.

3. REGULARIZATION OF $G_i(\xi, \eta)$

As has been discussed previously, the integrand $G_i(\xi, \eta)$ is strongly singular with an order O^{-1}. In terms of the local coordinates, the associated integral is rewritten as

$$I_i = \int_{-1}^{1}\int_{-1}^{1} \frac{N^{(i)}(\xi,\eta)\, J(\xi,\eta)}{\sqrt{D(\xi,\eta)}}\, d\xi\, d\eta, \quad (10)$$

where, for a quadratic element, $D(\xi, \eta)$ is a polynomial written as

$$D(\xi, \eta) = \sum_{l=1}^{3}\left(\sum_{c=1}^{k} N^{(c)} x_l^{(c)} - xp_l\right)^2 = \sum_{n=0}^{4} A_n(\eta)\xi^n = \sum_{n=0}^{4} B_n(\xi)\eta^n. \quad (11)$$

https://doi.org/10.1017/jmech.2012.140 Published online by Cambridge University Press

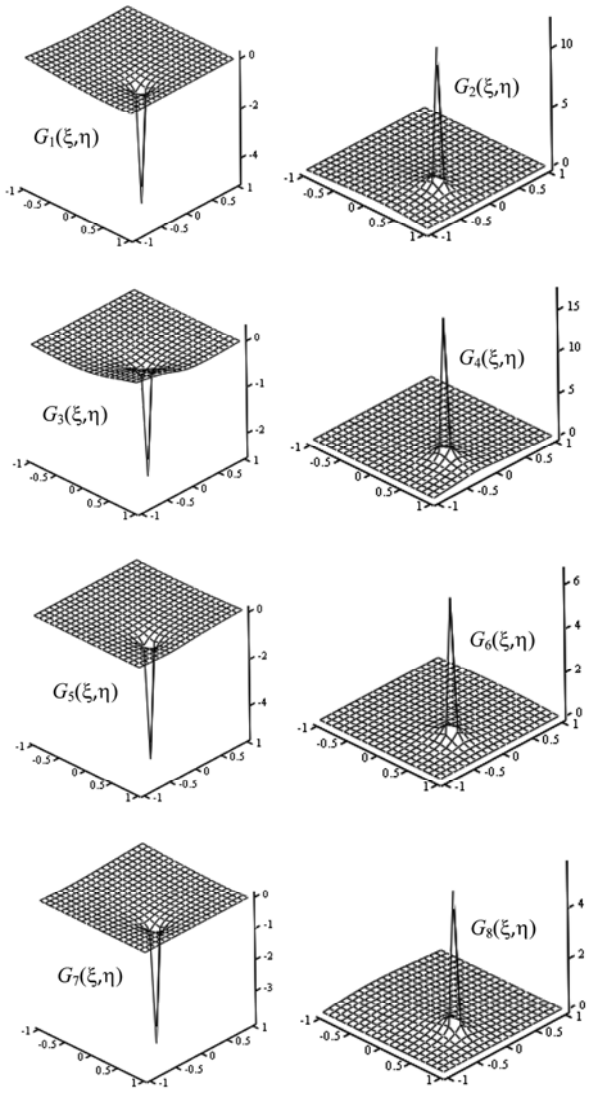


Fig. 2 Fluctuations of the integrands $G_i(\xi, \eta)$

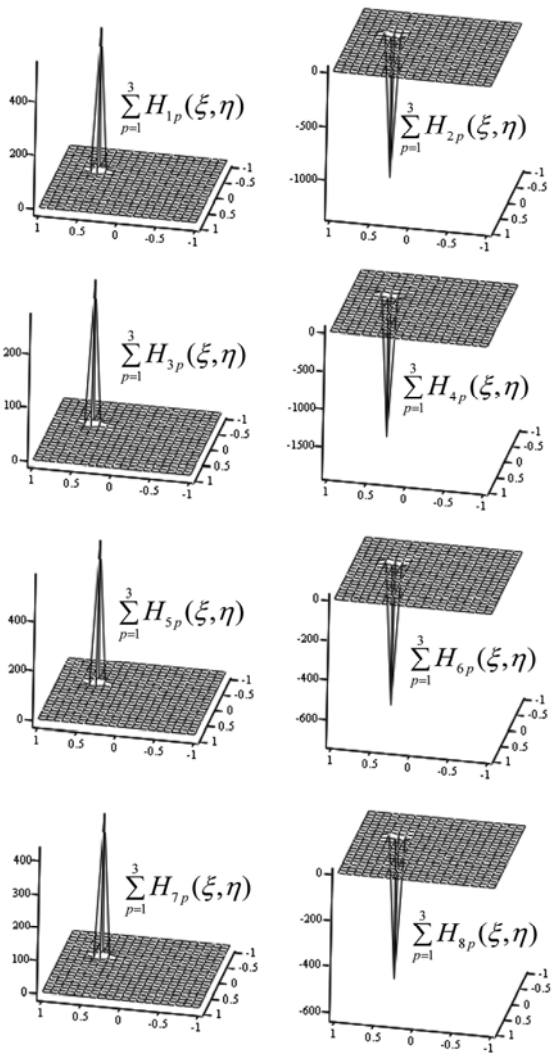


Fig. 3 Fluctuations of the integrands $\sum_{p=1}^{3} H_{ip}(\xi, \eta)$

For general quadratic elements, both $A_n(\eta)$ and $B_n(\xi)$ in Eq. (11) are quartic equations expressed as

$$A_n(\eta) = \sum_{m=0}^{4} E_{mn}\, \eta^m \ , \quad B_n(\xi) = \sum_{m=0}^{4} F_{mn}\, \xi^m \ , \tag{12}$$

where both E_{mn} and F_{mn} are constants associated with nodal coordinates of the element and the source coordinates as well. Since they can be easily formulated by simple algebraic operations, their very explicit formulations are not provided herein. One should keep in mind that when the source point approaches the element under integration, the value of $D(\xi, \eta)$ will become very small (near null) and thus invalidate any conventional numerical integration schemes.

Before further treatment of the integrand, one needs to locate the projected point (ξ_0, η_0) of the source on the element, resulting in the minimum $D(\xi, \eta)$. Under this condition, one has

$$D_{,\xi}(\xi_0, \eta_0) = \left.\frac{\partial D(\xi, \eta)}{\partial \xi}\right|_{\substack{\xi=\xi_0 \\ \eta=\eta_0}} = 0 \ ,$$

$$D_{,\eta}(\xi_0, \eta_0) = \left.\frac{\partial D(\xi, \eta)}{\partial \eta}\right|_{\substack{\xi=\xi_0 \\ \eta=\eta_0}} = 0 \tag{13}$$

Taking partial differentiations of $D(\xi, \eta)$ with respect to ξ and η using Eq. (11) leads to two simultaneous equations,

$$\sum_{n=1}^{4} n\, A_n(\eta_0)\xi_0^{\,n-1} = 0 \ , \quad \sum_{n=1}^{4} n\, B_n(\xi_0)\eta_0^{\,n-1} = 0 \ . \tag{14}$$

Recall both $A_n(\eta)$ and $B_n(\xi)$ are quartic equations and, thus, analytically solving the above simultaneous equations is not an easy task by any means. In an iterative manner, one may give an initial guess value of ξ, denote by ξ_1, and substitute it in the second equation to give a cubic equation of η_1, *i.e.*

$$\sum_{n=1}^{4} n\, B_n(\xi_1)\eta_1^{\,n-1} = 0 \ , \tag{15}$$

https://doi.org/10.1017/jmech.2012.140 Published online by Cambridge University Press

which can be solved for η_1 either analytically or numerically. It should be noted that only one real root $\eta_1 \in [-1, 1]$ is accepted as the useful value and the rest roots are discarded. As a sequential step, the obtained value for η_1 is substituted into the other equation so that

$$\sum_{n=1}^{4} n\, A_n(\eta_1)\xi_2^{\,n-1} = 0 \,, \tag{16}$$

which can be analytically or numerically solved like before to obtain ξ_2. The same processes can be iteratively carried out by solving

$$\sum_{n=1}^{4} n\, B_n(\xi_k)\eta_k^{\,n-1} = 0 \,, \quad \sum_{n=1}^{4} n\, A_n(\eta_k)\xi_{k+1}^{\,n-1} = 0 \,. \tag{17}$$

to reach final convergent values for (ξ_0, η_0). Generally, convergence of such iterations may be achieved not exceeding ten times.

It should be noted that (ξ_0, η_0) must be bounded in the range of $[-1, 1]$ for nearly singular integrals. In case when no convergent values in $[-1, 1]$ can be founded, this integral is regular and can be numerically integrated by any conventional scheme. Up to this point so far, one may raise a concern regarding how to judge whether the integral needs regularizing treatment when programming a code. First, when no $(\xi_0, \eta_0) \in [-1, 1]$ can be founded, this integral is considered "regular". Once proper values of $(\xi_0, \eta_0) \in [-1, 1]$ are found through the iterations, one may then proceed to calculate

$$C_0 = \left| D(\xi_0, \eta_0) \right| / D_{\max} \,, \tag{18}$$

where $D_{\max}$ represents the maximum absolute value of $D(\xi, \eta)$ for all element nodes. When C_0 is smaller than a small critical value δ decided in advance by the user (*i.e.* $C_0 < \delta$), then this integral is considered "nearly singular".

In principal, the integrand $C_i(\xi, \eta)$ may be regularized by the scheme of integration by parts as has been achieved previously for 2D cases [16]. There are two ways to regularize the integral by the scheme of integration by parts. The first approach is to rewrite the integral as

$$I_i = \int_{-1}^{1}\int_{-1}^{1} \frac{N^{(i)}(\xi, \eta)\, J(\xi, \eta)\sqrt{\xi - \xi_0}}{\sqrt{D(\xi, \eta)}} \frac{1}{\sqrt{\xi - \xi_0}}\, d\xi\, d\eta \,. \tag{19}$$

By letting

$$U(\xi, \eta) = \frac{N^{(i)}(\xi, \eta)\, J(\xi, \eta)\sqrt{\xi - \xi_0}}{\sqrt{D(\xi, \eta)}}, \qquad dV(\xi) = \frac{1}{\sqrt{\xi - \xi_0}}\, d\xi \tag{20}$$

and applying the technique of integration by parts,

$$\int_{-1}^{1} U\, dV\, d\xi = U\, V\Big|_{\xi=-1}^{\xi=1} - \int_{-1}^{1} V\, dU\, d\xi \,, \tag{21}$$

one has

$$\begin{aligned} I_i = & \int_{-1}^{1} \frac{2N^{(i)} J(\xi - \xi_0)}{\sqrt{D(\xi, \eta)}}\Bigg|_{\xi=-1}^{\xi=1} d\eta \\ & - \int_{-1}^{1}\int_{-1}^{1} \frac{2(\xi - \xi_0)\overline{NJ}^{(i)}(\xi, \eta)}{\sqrt{D(\xi, \eta)}}\, d\xi\, d\eta \\ & - \int_{-1}^{1}\int_{-1}^{1} \frac{N^{(i)}(\xi, \eta) J(\xi, \eta)}{\sqrt{D(\xi, \eta)}}\, d\xi\, d\eta \\ & + \int_{-1}^{1}\int_{-1}^{1} \frac{(\xi - \xi_0) N^{(i)}(\xi, \eta) J(\xi, \eta)\, D_{,\xi}(\xi, \eta)}{\sqrt{D(\xi, \eta)^3}}\, d\xi\, d\eta \,, \end{aligned} \tag{22}$$

where $\overline{NJ}^{(i)}(\xi, \eta)$ is defined by

$$\overline{NJ}^{(i)}(\xi, \eta) = \frac{\partial N^{(i)}(\xi, \eta)}{\partial \xi} J(\xi, \eta) + N^{(i)}(\xi, \eta) \frac{\partial J(\xi, \eta)}{\partial \xi} \,. \tag{23}$$

By further checking the third integral in Eq. (22), one may immediately tell it is identical with the original I_i and, thus, rearrangement of Eq. (22) yields

$$\begin{aligned} I_i = & \int_{-1}^{1} \frac{(\xi - \xi_0) N^{(i)} J}{\sqrt{D}}\Bigg|_{\xi=-1}^{\xi=1} d\eta \\ & - \int_{-1}^{1}\int_{-1}^{1} \frac{(\xi - \xi_0)\overline{NJ}^{(i)}}{\sqrt{D}}\, d\xi\, d\eta \\ & + \int_{-1}^{1}\int_{-1}^{1} \frac{(\xi - \xi_0) N^{(i)} J\, D_{,\xi}}{2\sqrt{D^3}}\, d\xi\, d\eta \,, \end{aligned} \tag{24}$$

where the function variables of the local coordinates (ξ, η) are omitted for conciseness. Apparently, under the circumstance when the source point approaches its projection point (ξ_0, η_0), the sharp spikes of the integrand values will be suppressed by the presence of $(\xi - \xi_0)$ in the numerator. It is noted that although the last integral has a stronger singularity than the others, it can still be properly integrated due to the condition in Eq. (13), *i.e.* $D_{,\xi}(\xi_0, \eta_0) = 0$. Strictly speaking, this integral is only partially regularized because, for arbitrary ξ falling outside the vicinity of ξ_0, the condition when η approaches η_0 will still yield relatively small values for the denominator, but not fluctuating so drastically like the original. For providing a remedy to resolve this issue, the integral domain is sub-divided into sub-domains in a manner as follows:

https://doi.org/10.1017/jmech.2012.140 Published online by Cambridge University Press

$$
\begin{aligned}
I_i = & \int_{-1}^{\eta_0} \frac{(\xi-\xi_0)N^{(i)}J}{\sqrt{D}}\bigg|_{\xi=-1}^{\xi=1} d\eta + \int_{\eta_0}^{1} \frac{(\xi-\xi_0)N^{(i)}J}{\sqrt{D}}\bigg|_{\xi=-1}^{\xi=1} d\eta \\
& - \int_{-1}^{\eta_0}\int_{-1}^{\xi_0} \frac{(\xi-\xi_0)\overline{NJ}^{(i)}}{\sqrt{D}}\, d\xi d\eta - \int_{-1}^{\eta_0}\int_{\xi_0}^{1} \frac{(\xi-\xi_0)\overline{NJ}^{(i)}}{\sqrt{D}}\, d\xi d\eta \\
& - \int_{\eta_0}^{1}\int_{\xi_0}^{1} \frac{(\xi-\xi_0)\overline{NJ}^{(i)}}{\sqrt{D}}\, d\xi d\eta - \int_{\eta_0}^{1}\int_{\xi_0}^{1} \frac{(\xi-\xi_0)\overline{NJ}^{(i)}}{\sqrt{D}}\, d\xi d\eta \\
& + \int_{-1}^{\eta_0}\int_{-1}^{\xi_0} \frac{(\xi-\xi_0)N^{(i)}J\,D_{,\xi}}{2\sqrt{D^3}}\, d\xi d\eta - \int_{-1}^{\eta_0}\int_{\xi_0}^{1} \frac{(\xi-\xi_0)N^{(i)}J\,D_{,\xi}}{2\sqrt{D^3}}\, d\xi d\eta \\
& + \int_{\eta_0}^{1}\int_{\xi_0}^{1} \frac{(\xi-\xi_0)N^{(i)}J\,D_{,\xi}}{2\sqrt{D^3}}\, d\xi d\eta + \int_{\eta_0}^{1}\int_{\xi_0}^{1} \frac{(\xi-\xi_0)N^{(i)}J\,D_{,\xi}}{2\sqrt{D^3}}\, d\xi d\eta \,.
\end{aligned} \tag{25}
$$

For verifying the validity of the regularized forms, a test case is investigated that considers a quadrilateral element with the following nodes ($r^{(i)}$, $\theta^{(i)}$, $\phi^{(i)}$) and the source point (r_p, θ_p, ϕ_p) defined in the spherical coordinates:

$$
\begin{aligned}
& r^{(1)}=1.0\,,\ \theta^{(1)}=\pi/6\,,\ \phi^{(1)}=\pi/3\,,\ r^{(2)}=1.0\,,\ \theta^{(2)}=\pi/4\,,\ \phi^{(2)}=\pi/3\,, \\
& r^{(3)}=1.0\,,\ \theta^{(3)}=\pi/3\,,\ \phi^{(3)}=\pi/3\,,\ r^{(4)}=1.0\,,\ \theta^{(4)}=\pi/3\,,\ \phi^{(4)}=\pi/4\,, \\
& r^{(5)}=1.0\,,\ \theta^{(5)}=\pi/3\,,\ \phi^{(5)}=\pi/6\,,\ r^{(6)}=1.0\,,\ \theta^{(6)}=\pi/4\,,\ \phi^{(6)}=\pi/6\,, \\
& r^{(7)}=1.0\,,\ \theta^{(7)}=\pi/6\,,\ \phi^{(7)}=\pi/6\,,\ r^{(8)}=1.0\,,\ \theta^{(8)}=\pi/6\,,\ \phi^{(8)}=\pi/4\,, \\
& r_p=1.0-\delta\,,\ \theta_p=0.292\pi\,,\ \phi_p=0.275\pi\,,
\end{aligned} \tag{26}
$$

Table 1 Numerical values of I_i for the test case

		$\delta=10^{-1}$	$\delta=10^{-2}$	$\delta=10^{-3}$	$\delta=10^{-5}$	$\delta=10^{-7}$
$i=1$	MathCAD	–0.101732	–0.168495	–0.178210	–0.178064	–0.178051
	Gauss Intg. (original)	–0.101732 (0.00%)	–0.182284 (8.18%)	–0.239487 (34.38%)	–0.239236 (34.35%)	–0.239205 (34.35%)
	Gauss Intg. (Eq.(25))	–0.101732 (0.00%)	–0.168502 (0.00%)	–0.178216 (0.00%)	–0.178094 (0.02%)	–0.178085 (0.02%)
	Gauss Intg. (Eq.(37))	–0.101761 (0.03%)	–0.168518 (0.01%)	–0.178061 (0.08%)	–0.177943 (0.07%)	–0.177936 (0.07%)
$i=2$	MathCAD	0.397220	0.578913	0.602861	0.602415	0.602381
	Gauss Intg. (original)	0.397221 (0.00%)	0.614126 (6.08%)	0.758605 (25.83%)	0.757896 (25.81%)	0.757817 (25.80%)
	Gauss Intg. (Eq.(25))	0.397220 (0.00%)	0.578931 (0.00%)	0.602870 (0.00%)	0.602485 (0.01%)	0.602463 (0.01%)
	Gauss Intg. (Eq.(37))	0.397274 (0.01%)	0.578923 (0.00%)	0.602432 (0.07%)	0.602059 (0.06%)	0.602040 (0.06%)
$i=3$	MathCAD	–0.070320	–0.097487	–0.101914	–0.101834	–0.101828
	Gauss Intg. (original)	–0.070320 (0.00%)	–0.103028 (5.68%)	–0.127642 (25.25%)	–0.127520 (25.22%)	–0.127507 (25.22%)
	Gauss Intg. (Eq.(25))	–0.070320 (0.00%)	–0.097491 (0.00%)	–0.101915 (0.00%)	–0.101846 (0.01%)	–0.101842 (0.01%)
	Gauss Intg. (Eq.(37))	–0.070298 (0.03%)	–0.097467 (0.02%)	–0.101813 (0.10%)	–0.101749 (0.09%)	–0.101743 (0.08%)
$i=4$	MathCAD	0.399577	0.641889	0.676403	0.675865	0.675819
	Gauss Intg. (original)	0.399577 (0.00%)	0.691007 (7.65%)	0.894615 (32.26%)	0.893708 (32.23%)	0.893599 (32.22%)
	Gauss Intg. (Eq.(25))	0.399577 (0.00%)	0.641912 (0.00%)	0.676440 (0.01%)	0.675989 (0.02%)	0.675960 (0.02%)
	Gauss Intg. (Eq.(37))	0.399705 (0.03%)	0.641948 (0.01%)	0.675845 (0.08%)	0.675411 (0.07%)	0.675385 (0.06%)
$i=5$	MathCAD	–0.111920	–0.182961	–0.193460	-0.193301	–0.193287
	Gauss Intg. (original)	–0.111920 (0.00%)	–0.197976 (8.21%)	–0.259997 (34.39%)	–0.259726 (34.36%)	–0.259693 (34.36%)
	Gauss Intg. (Eq.(25))	–0.111920 (0.00%)	–0.182968 (0.00%)	–0.193468 (0.00%)	–0.193335 (0.02%)	–0.193326 (0.02%)
	Gauss Intg. (Eq.(37))	–0.111905 (0.01%)	–0.182940 (0.01%)	–0.193252 (0.11%)	–0.193124 (0.09%)	–0.193116 (0.09%)
$i=6$	MathCAD	0.282659	0.379992	0.392457	0.392184	0.392167
	Gauss Intg. (original)	0.282659 (0.00%)	0.397648 (4.65%)	0.471956 (20.26%)	0.471550 (20.24%)	0.471509 (20.23%)
	Gauss Intg. (Eq.(25))	0.282659 (0.00%)	0.380001 (0.00%)	0.392466 (0.00%)	0.392226 (0.01%)	0.392214 (0.01%)

https://doi.org/10.1017/jmech.2012.140 Published online by Cambridge University Press

	Gauss Intg. (Eq.(37))	0.282717 (0.02%)	0.380018 (0.01%)	0.392252 (0.05%)	0.392018 (0.04%)	0.392008 (0.04%)
$i = 7$	MathCAD	–0.110030	–0.166669	–0.174385	–0.174251	–0.174241
	Gauss Intg. (original)	–0.110030 (0.00%)	–0.177454 (6.47%)	–0.222660 (27.68%)	–0.222446 (27.66%)	–0.222421 (27.65%)
	Gauss Intg. (Eq.(25))	–0.110030 (0.00%)	–0.166674 (0.00%)	–0.174390 (0.00%)	–0.174276 (0.01%)	–0.174269 (0.02%)
	Gauss Intg. (Eq.(37))	–0.110041 (0.01%)	–0.166664 (0.00%)	–0.174242 (0.08%)	–0.174131 (0.07%)	–0.174125 (0.07%)
$i = 8$	MathCAD	0.306987	0.397788	0.408393	0.408122	0.408106
	Gauss Intg. (original)	0.306987 (0.00%)	0.413306 (3.90%)	0.477814 (17.00%)	0.477427 (16.98%)	0.477391 (16.98%)
	Gauss Intg. (Eq.(25))	0.306987 (0.00%)	0.397796 (0.00%)	0.408397 (0.00%)	0.408154 (0.01%)	0.408143 (0.01%)
	Gauss Intg. (Eq.(37))	0.306988 (0.00%)	0.397737 (0.01%)	0.408138 (0.06%)	0.407901 (0.05%)	0.407892 (0.05%)

where δ represents a small radial distance away from the element surface. The original integral is evaluated using Gauss Quadrature scheme by 14 points and additionally by the MathCAD, a mathematic software package capable of computing improper integrals accurately. Generally, speaking, numerical integration of regular integrals may use fewer points of the Gauss Quadrature scheme. This may apply to the present cases when δ is larger than 10^{-2}; however, relatively more Gauss points are needed for smaller δ due to the fluctuations of integrands of the present regularized forms. For assuring numerical convergence for smaller δ (up to 10^{-7} in our tests), 14-point Gauss Quadrature scheme is applied throughout our numerical tests. For various δ being gradually decreased from 10^{-1} to 10^{-7}, Table 1 lists the computed results. Since no other reliable numerical schemes are available for such analyses, the numerical values of MathCAD served as the comparison platform. From Tab.1, it is apparent to see that no matter how small the distance is, computing Eq. (25) by the Gauss 14-point scheme can always yield proper values with satisfactory accuracies, while integration of the original form does not.

The other approach for the general case when $A_4 \neq 0$ is to rewrite the integral as

$$I_i = \int_{-1}^{1}\int_{-1}^{1} \frac{N^{(i)}\, J}{\sqrt{A_4}\sqrt{\xi^4 + f_3\,\xi^3 + f_2\,\xi^2 + f_1\,\xi + f_0}}\, d\xi\, d\eta\ , \tag{27}$$

where f_i is defined by

$$f_i = A_i / A_4\ . \tag{28}$$

For the degenerate case when $A_4 = 0$ occurs, the similar process can be applied and thus no further details for treating the special case are provided. In what follows, treatment is taken only for the general case when $A_4 \neq 0$. According to the Ferrari's theory [19], any quartic equation can be analytically factored into four terms and, thus, Eq. (27) is rewritten as

$$\begin{aligned} I_i &= \int_{-1}^{1}\int_{-1}^{1} \frac{N^{(i)}\, J}{\sqrt{A_4}\sqrt{(\xi - X_1)(\xi - X_2)(\xi - X_3)(\xi - X_4)}}\, d\xi\, d\eta \\ &= \int_{-1}^{1}\int_{-1}^{1} \frac{N^{(i)}(\xi,\eta)\, J(\xi,\eta)}{\sqrt{A_4}\sqrt{(\xi^2 + \alpha_1\xi + \alpha_0)(\xi^2 + \beta_1\xi + \beta_0)}}\, d\xi\, d\eta\ , \end{aligned} \tag{29}$$

where

$$\alpha_0 = X_1\, X_2,\ \alpha_1 = -X_1 - X_2,\ \beta_0 = X_3\, X_4,\ \beta_1 = -X_3 - X_4\ . \tag{30}$$

In Eq. (29), it should be noted that A_4, $X_1 \sim X_4$, α_0, α_1, β_0, and β_1 are all functions of η and, for conciseness, the implicit variables (ξ, η) are omitted in all derivations from now on. The reader may be referred to [20] for the explicit formulations of $X_i(\eta)$. It is worth pointing out that, at the projection point (ξ_0, η_0), ($\xi_0 - X_i(\eta_0)$) are present as two pairs of conjugated complex values. Under the nearly singular condition, the product of one pair of them, called the ill term, turns out to be very small. The ill term can be easily identified in a computer code by checking the values of ($\xi_0 - X_i(\eta_0)$). Suppose $X_1(\eta)$ and $X_2(\eta)$ are the ones leading to the nearly singular condition, *i.e.* $\xi_0^2 + \alpha_1(\eta_0)\xi_0 + \alpha_0(\eta_0) \approx 0$. Let

$$U^{(i)} = \frac{N^{(i)}\, J}{\sqrt{A_4}\sqrt{\xi^2 + \beta_1\xi + \beta_0}},\quad dV = \frac{d\xi}{\sqrt{\xi^2 + \alpha_1\xi + \alpha_0}}\ , \tag{31}$$

one may obtain

$$\begin{aligned} dU^{(i)} &= \frac{1}{\sqrt{A_4}}\left(\frac{\overline{NJ}^{(i)}}{\sqrt{\xi^2 + \beta_1\xi + \beta_0}} - \frac{N^{(i)} J\,(2\xi + \beta_1)}{2\sqrt{(\xi^2 + \beta_1\xi + \beta_0)^3}}\right) d\xi \\ V &= \ln\left(\xi + \frac{\alpha_1}{2} + \sqrt{\xi^2 + \alpha_1\xi + \alpha_0}\right)\ . \end{aligned} \tag{32}$$

and, therefore, directly applying the scheme of integration by parts for ξ yields

$$\begin{aligned} I_i = &\int_{-1}^{1} U^{(i)} \ln\left(\xi + \frac{\alpha_1}{2} + \sqrt{\xi^2 + \alpha_1\xi + \alpha_0}\right)\Bigg|_{\xi=-1}^{\xi=1} d\eta \\ &- \int_{-1}^{1}\int_{-1}^{1} f^{(i)} \ln\left(\xi + \frac{\alpha_1}{2} + \sqrt{\xi^2 + \alpha_1\xi + \alpha_0}\right) d\xi\, d\eta\ , \end{aligned} \tag{33}$$

where $f^{(i)}$ is defined by

$$f^{(i)} = \frac{1}{\sqrt{A_4}}\left(\frac{\overline{NJ}^{(i)}}{\sqrt{\xi^2 + \beta_1\xi + \beta_0}} - \frac{N^{(i)} J\,(2\xi + \beta_1)}{2\sqrt{(\xi^2 + \beta_1\xi + \beta_0)^3}}\right)\ . \tag{34}$$

https://doi.org/10.1017/jmech.2012.140 Published online by Cambridge University Press

Since $X_3(\eta)$ and $X_4(\eta)$ both behave well within the whole integration range, their associated functions shall not give rise to any ill condition at (ξ_0, η_0). However, the double integral in Eq. (33) still reveals weak singularity in the logarithmic manner when the source point approaches (ξ_0, η_0). Full regularization of this integral requires applying the integration by parts again. For this time, assume

$$U^{(i)} = f^{(i)}, \quad dV = \ln\left(\xi + \frac{\alpha_1}{2} + \sqrt{\xi^2 + \alpha_1\xi + \alpha_0}\right) d\xi \ . \quad (35)$$

and, therefore, direct differentiation of $U(\xi, \eta)$ and integration of $dV(\xi, \eta)$ with respect to ξ yields

$$dU^{(i)} = \frac{1}{\sqrt{A_4}}\left(\frac{\overline{NJ}_\xi^{(i)}}{\sqrt{\xi^2 + \beta_1\xi + \beta_0}} + \frac{3N^{(i)}J\,(2\xi + \beta_1)}{4\sqrt{(\xi^2 + \beta_1\xi + \beta_0)^5}} - \frac{\overline{NJ}^{(i)}(2\xi + \beta_1) + N^{(i)}J}{\sqrt{(\xi^2 + \beta_1\xi + \beta_0)^5}}\right) d\xi$$

$$V = -\sqrt{\xi^2 + \alpha_1\xi + \alpha_0} + \left(\xi + \frac{\alpha_1}{2}\right) \ln\left(\xi + \frac{\alpha_1}{2} + \sqrt{\xi^2 + \alpha_1\xi + \alpha_0}\right) , \quad (36)$$

where $\overline{NJ}_\xi^{(i)}$ represents taking partial differentiation of $\overline{NJ}^{(i)}$ with respect to ξ, *i.e.*

$$\overline{NJ}_\xi^{(i)} = \frac{\partial^2 N^{(i)}}{\partial\xi^2}J + 2\frac{\partial N^{(i)}}{\partial\xi}\frac{\partial J}{\partial\xi} + N^{(i)}\frac{\partial^2 J}{\partial\xi^2} \ . \quad (37)$$

The explicit expression for $\overline{NJ}_\xi^{(i)}$ can be analytically obtained in a very straightforward manner. On applying the integration by parts, Eq. (33) is now rewritten as

$$I_i = \int_{-1}^{1} U^{(i)} \ln\left(\xi + \frac{\alpha_1}{2} + \sqrt{\xi^2 + \alpha_1\xi + \alpha_0}\right)\Bigg|_{\xi=-1}^{\xi=1} d\eta - \int_{-1}^{1} f^{(i)}\left[-\sqrt{\xi^2 + \alpha_1\xi + \alpha_0} + \left(\xi + \frac{\alpha_1}{2}\right) \ln\left(\xi + \frac{\alpha_1}{2} + \sqrt{\xi^2 + \alpha_1\xi + \alpha_0}\right)\right]\Bigg|_{\xi=-1}^{\xi=1} d\eta + \int_{-1}^{1}\int_{-1}^{1} g^{(i)}\left[-\sqrt{\xi^2 + \alpha_1\xi + \alpha_0} + \left(\xi + \frac{\alpha_1}{2}\right) \ln\left(\xi + \frac{\alpha_1}{2} + \sqrt{\xi^2 + \alpha_1\xi + \alpha_0}\right)\right] d\xi\, d\eta \ , \quad (38)$$

where $g^{(i)}$ is defined by

$$g^{(i)} = \frac{1}{\sqrt{A_4}}\left(\frac{\overline{NJ}_\xi^{(i)}}{\sqrt{\xi^2 + \beta_1\xi + \beta_0}} + \frac{3N^{(i)}J\,(2\xi + \beta_1)}{4\sqrt{(\xi^2 + \beta_1\xi + \beta_0)^5}} - \frac{\overline{NJ}^{(i)}\,(2\xi + \beta_1) + N^{(i)}J}{\sqrt{(\xi^2 + \beta_1\xi + \beta_0)^3}}\right) . \quad (39)$$

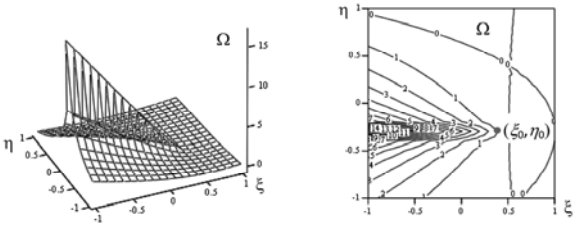
Under the near-singular circumstance, one may immediately tell that the double integral in Eq. (38) is a fully regularized form indeed. However, due to the fact that the logarithmic operation for $\xi < \xi_0$ yields large variation for η, the whole integrand still rapidly fluctuate for $\xi < \xi_0$ in the vicinity of η_0 (Fig. 4). Since the fluctuation is actually not so drastic for the regularized form, this integral can still be properly computed using the 14-point Gauss quadrature scheme for the sub-regions as in the previous approach. Table 1 also lists the numerical values computed by this approach for various distances of δ. It is interesting to see that when compared with MathCAD calculations, the numerical results by Eq. (38) have greater percentages of discrepancies than those computed by Eq. (25); however, the off-percentages for using Eq. (38) do not aggravate when the δ drops below 10^{-3}. As a matter of fact, the source of numerical errors when using Eq. (38) is mainly derived from computing the complex values of $X_1(\eta) \sim X_4(\eta)$ and their associated operations of mathematical functions. In general, the former approach using $(\xi - \xi_0)$ as the regularization factor is concluded to be more efficient and accurate as compared with the latter.

4. REGULARIZATION OF $H_{IS}(\xi, \eta)$

As discussed earlier, the integral associated with $H_{is}(\xi, \eta)$, denoted by K_{is} herein, is quasi-hypersingular when the source is very close the element under integration. In this section, the effort is dedicated to applying the previous approaches to regularize K_{is} so that the usual numerical integration scheme may correctly compute the integral. As the first attempt, the former scheme using the regularizing factor $(\xi - \xi_0)$ was employed again for regularizing K_{is}. Unfortunately, this attempt did not succeed in overcoming the quasi-hypersingularity. Alternatively, the other approach is applied for the regularization process, which will be elaborated in the following.

Suppose $X_1(\eta)$ and $X_2(\eta)$ are ill conjugated terms leading to the near-singularity. Omitting implicit variables of functions for conciseness, K_{is} can be rewritten as

$$K_{is} = \int_{-1}^{1}\int_{-1}^{1} \frac{\left(xp_i - \sum_{c=1}^{k} N^{(c)}x_i^{(c)}\right)N^{(s)}\,J_i}{\sqrt{A_4^3}\sqrt{(\xi^2 + \beta_1\xi + \beta_0)^3}} \cdot \frac{1}{\sqrt{(\xi^2 + \alpha_1\xi + \alpha_0)^3}}\, d\xi\, d\eta \ , \quad (40)$$



(a) Surface plot (b) Contour plot

Fig. 4 Variation of $\Omega(\xi, \eta)$: (a) surface plot, (b) contour plot

https://doi.org/10.1017/jmech.2012.140 Published online by Cambridge University Press

where α_0, α_1, β_0, and β_1 are defined by

$$\alpha_0 = X_1 X_2 \ , \alpha_1 = -X_1 - X_2 \ , \beta_0 = X_3 X_4 \ , \beta_1 = -X_3 - X_4 \ . \tag{41}$$

By applying the technique of integration by parts with

$$\begin{aligned} U &= \frac{\left(xp_i - \sum_{c=1}^{k} N^{(c)} x_i^{(c)} \right) N^{(s)} J_i}{\sqrt{A_4^3 \sqrt{(\xi^2 + \beta_1 \xi + \beta_0)^3}}} \ , \\ dV &= \frac{1}{\sqrt{(\xi^2 + \alpha_1 \xi + \alpha_0)^3}} d\xi \ , \end{aligned} \tag{42}$$

one will obtain

$$\begin{aligned} K_{is} = & \int_{-1}^{1} \frac{-2 N^{(s)} J_i (2\xi + \alpha_1) \left(xp_i - \sum_{c=1}^{k} N^{(c)} x_i^{(c)} \right)}{(X_1 - X_2)^2 \sqrt{A_4^3} \sqrt{\xi^2 + \alpha_1 \xi + \alpha_0} \sqrt{(\xi^2 + \beta_1 \xi + \beta_0)^3}} \Bigg|_{\xi=-1}^{\xi=1} d\eta \\ & - \int_{-1}^{1} \int_{-1}^{1} \frac{2\xi + \alpha_1}{(X_1 - X_2)^2 \sqrt{A_4^3} \sqrt{\xi^2 + \alpha_1 \xi + \alpha_0}} \left(\begin{array}{l} \dfrac{2 N^{(s)} J_i \sum_{c=1}^{k} N_{,\xi}^{(c)} x_i^{(c)} - 2 \left(xp_i - \sum_{c=1}^{k} N^{(c)} x_i^{(c)} \right) NJ'_{is}}{\sqrt{(\xi^2 + \beta_1 \xi + \beta_0)^3}} \\ + \dfrac{3 N^{(s)} J_i (xp_i - \sum_{c=1}^{k} N^{(c)} x_i^{(c)})(2\xi + \beta_1)}{\sqrt{(\xi^2 + \beta_1 \xi + \beta_0)^5}} \end{array} \right) d\xi d\eta \ , \end{aligned} \tag{43}$$

where NJ'_{is} is defined by

$$NJ'_{is} = \frac{\partial N^{(s)}}{\partial \xi} J_i + N^{(s)} \frac{\partial J_i}{\partial \xi} \ . \tag{44}$$

when the distance between the source point and its projection point (ξ_0 ,η_0) approaches null, one will have

$$2\xi_0 + \alpha_1(\eta_0) \approx 0 \ , \quad \xi_0^2 + \alpha_1(\eta_0)\, \xi_0 + \alpha_0(\eta_0) \approx 0 \ . \tag{45}$$

On applying the above conditions to Eq. (43), one might have an impression that all integrals are regular; however, this is not true. This is due to the fact that, under the nearly singular condition, the ill terms $X_{1/2}(\eta_0)$ are complex conjugates, written as

$$X_{1/2}(\eta_0) = \eta_0 \pm \Delta\, i \ , \tag{46}$$

where "i" denotes $\sqrt{-1}$ and Δ is a small number approaching null. Obviously, another ill condition, $X_1(\eta_0) - X_2(\eta_0) \approx 0$ in the denominator, arises and invalidates regular numerical integration; otherwise, all other terms behave regularly. It is interesting to see that, although the singularity order O^{-2} still exists, the quasi-singular terms depends now on η only. With no doubt, this process has eased the difficulty of regularization in the halfway. Despite their complicated formulations, $X_{1/2}(\eta)$ are smooth functions of η and the function $(X_1(\eta) - X_2(\eta))^2$ can be approximately represented by a Taylor series in the vicinity of η_0. However, being the main drawback of this approach, the approximation accuracy is susceptible to the choice of the vicinity range. To attain accuracy insensitive to the vicinity range, higher-order Taylor's series may be required. In the present study, the approximation employs the 4-order Taylor's series at η_0, *i.e.*

$$\begin{aligned} f(\eta) &= \left(X_1(\eta) - X_2(\eta) \right)^2 \\ &\cong \sum_{i=0}^{4} c_i \eta^i \\ &= c_4 (\eta - \lambda_1)(\eta - \lambda_2)(\eta - \lambda_3)(\eta - \lambda_4) \ , \end{aligned} \tag{47}$$

where the constants c_i are defined by

https://doi.org/10.1017/jmech.2012.140 Published online by Cambridge University Press

$$c_4 = \frac{f^{(4)}(\eta_0)}{24}\ ,\ c_3 = \frac{f^{(3)}(\eta_0) - \eta_0 f^{(4)}(\eta_0)}{6}\ ,\ c_2 = \frac{\eta_0^2 f^{(4)}(\eta_0)}{4} - \frac{\eta_0 f^{(3)}(\eta_0)}{2} + \frac{f^{(2)}(\eta_0)}{2}\ ,$$
$$c_1 = -\frac{\eta_0^3 f^{(4)}(\eta_0)}{6} + \frac{\eta_0^2 f^{(3)}(\eta_0)}{2} - \eta_0 f^{(2)}(\eta_0) + f^{(1)}(\eta_0)\ , \tag{48}$$
$$c_0 = \frac{\eta_0^4 f^{(4)}(\eta_0)}{24} - \frac{\eta_0^3 f^{(3)}(\eta_0)}{6} + \frac{\eta_0^2 f^{(2)}(\eta_0)}{2} - \eta_0 f^{(1)}(\eta_0) + f(\eta_0)\ ,$$

and $\lambda_1 \sim \lambda_4$ are the four roots of the polynomial that can be determined either analytically or numerically. For the example case defined in Eqs. (26) with $\delta = 10^{-5}$, Fig. 5 shows the variations of $(X_1 - X_2)^2$ and its 4-order Taylor's series Eq. (47). It should be noted that, for general cases, $\lambda_1 \sim \lambda_4$ are two distinct pairs of complex conjugates. For the degenerate case when repeated roots occur, the process is similar to the general case and, thus, no special treatment for the degenerate case will be discussed. Note that the Taylor's expansion holds true only in the vicinity of η_0 bounded by $[\eta_0 - \delta,\ \eta_0 + \delta]$, where δ is a small value. Since the integrands in Eq. (43) behave regularly outside the small bound, the integral in Eq. (43) can be separated into two parts- one inside the bound and the other outside the bound. First, the integral is expressed as

$$K_{is} = \int_{-1}^{1} \omega_i^{(s)}(\eta)\, d\eta - \int_{-1}^{1}\int_{-1}^{1} \Omega_i^{(s)}(\xi,\eta)\, d\xi\, d\eta\ , \tag{49}$$

where $\omega_i^{(s)}(\eta)$ and $\Omega_i^{(s)}(\xi,\eta)$, abbreviated respectively as $\omega_i^{(s)}$ and $\Omega_i^{(s)}$, are defined by

$$\omega_i^{(s)} = \left. \frac{-2\, N^{(s)} J_i (2\xi + \alpha_1)\left(xp_i - \sum_{c=1}^{k} N^{(c)} x_i^{(c)} \right)}{(X_1 - X_2)^2 \sqrt{A_4^3}\sqrt{\xi^2 + \alpha_1\xi + \alpha_0}\sqrt{(\xi^2 + \beta_1\xi + \beta_0)^3}} \right|_{\xi=-1}^{\xi=1}\ , \tag{50a}$$

$$\Omega_i^{(s)} = \frac{2\xi + \alpha_1}{(X_1 - X_2)^2 \sqrt{A_4^3}\sqrt{\xi^2 + \alpha_1\xi + \alpha_0}} \left(\begin{array}{l} \dfrac{2N^{(s)} J_i \sum_{c=1}^{k} N_\xi^{(c)} x_i^{(c)} - 2\left(xp_i - \sum_{c=1}^{k} N^{(c)} x_i^{(c)} \right) NJ'_{is}}{\sqrt{(\xi^2 + \beta_1\xi + \beta_0)^3}} \\ + \dfrac{3N^{(s)} J_i \left(xp_i - \sum_{c=1}^{k} N^{(c)} x_i^{(c)} \right)(2\xi + \beta_1)}{\sqrt{(\xi^2 + \beta_1\xi + \beta_0)^5}} \end{array} \right)\ . \tag{50b}$$

Consider the above integrand in Eq. (50b), rewritten as

$$\Omega_i^{(s)} = \frac{\Theta_i^{(s)}}{(X_1 - X_2)^2}, \tag{51}$$

where $\Theta_i^{(s)}$ is defined by

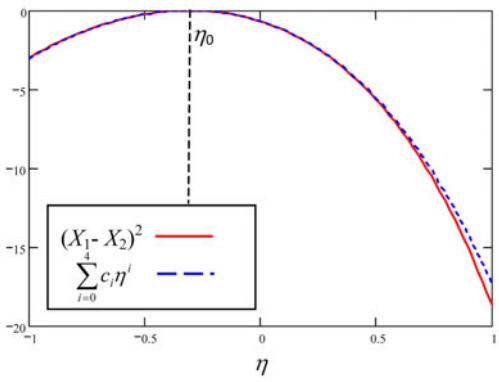


Fig. 5 Taylor's series approximation of $(X_1 - X_2)^2$ for the example case when $\delta = 10^{-5}$

https://doi.org/10.1017/jmech.2012.140 Published online by Cambridge University Press

$$\Theta_i^{(s)} = \frac{2\xi+\alpha_1}{\sqrt{A_4^3}\sqrt{\xi^2+\alpha_1\xi+\alpha_0}} \left(\begin{array}{l} \dfrac{2N^{(s)}J_i\sum\limits_{c=1}^{k} N_\xi^{(c)}x_i^{(c)} - 2\left(xp_i - \sum\limits_{c=1}^{k} N^{(c)}x_i^{(c)}\right)NJ'_{is}}{\sqrt{(\xi^2+\beta_1\xi+\beta_0)^3}} \\ + \dfrac{3N^{(s)}J_i(xp_i - \sum\limits_{c=1}^{k} N^{(c)}x_i^{(c)})(2\xi+\beta_1)}{\sqrt{(\xi^2+\beta_1\xi+\beta_0)^5}} \end{array} \right). \tag{52}$$

Note that although $\Theta_i^{(s)}$ is regular, further treatment of the function is still required. This is because when the process of integration by parts is performed later for dealing with the ill term by Eq. (47), differentiations of $\Theta_i^{(s)}$ with respect to η up to the 2nd order will be involved and, as a result, additional singularities will be introduced. For avoiding this, this double-integral must be integrated by parts twice with respect to ξ before its further treatment for regularization. The first integration by parts using Eq. (21) with

$$U = \frac{1}{\sqrt{A_4^3}(X_1-X_2)^2} \left(\begin{array}{l} \dfrac{2N^{(s)}J_i\sum\limits_{c=1}^{k} N_\xi^{(c)}x_i^{(c)} - 2\left(xp_i - \sum\limits_{c=1}^{k} N^{(c)}x_i^{(c)}\right)NJ'_{is}}{\sqrt{(\xi^2+\beta_1\xi+\beta_0)^3}} \\ + \dfrac{3N^{(s)}J_i\left(xp_i - \sum\limits_{c=1}^{k} N^{(c)}x_i^{(c)}\right)(2\xi+\beta_1)}{\sqrt{(\xi^2+\beta_1\xi+\beta_0)^5}} \end{array} \right), \tag{53a}$$

$$dV = \frac{2\xi+\alpha_1}{\sqrt{\xi^2+\alpha_1\xi+\alpha_0}}d\xi \ , \tag{53b}$$

results in

$$\begin{aligned} &\int_{-1}^{1}\int_{-1}^{1}\Omega_i^{(s)}(\xi,\ \eta)\,d\xi d\eta \\ &= 2\int_{-1}^{1}\frac{\sqrt{\xi^2+\alpha_1\xi+\alpha_0}}{(X_1-X_2)^2}\Gamma_i^{(s)}\Big|_{\xi=-1}^{\xi=1} d\eta - 2\int_{-1}^{1}\int_{-1}^{1}\frac{\sqrt{\xi^2+\alpha_1\xi+\alpha_0}}{(X_1-X_2)^2}\Gamma_i'^{(s)}d\xi d\eta\,, \end{aligned} \tag{54}$$

where $\Gamma_i^{(s)}$ is defined by

$$\Gamma_i^{(s)} = \frac{1}{\sqrt{A_4^3}} \left\{ \begin{array}{l} \dfrac{2N^{(s)}J_i\sum\limits_{c=1}^{k} N_\xi^{(c)}x_i^{(c)} - 2\left(xp_i - \sum\limits_{c=1}^{k} N^{(c)}x_i^{(c)}\right)NJ'_{is}}{\sqrt{(\xi^2+\beta_1\xi+\beta_0)^3}} \\ + \dfrac{3N^{(s)}J_i\left(xp_i - \sum\limits_{c=1}^{k} N^{(c)}x_i^{(c)}\right)(2\xi+\beta_1)}{\sqrt{(\xi^2+\beta_1\xi+\beta_0)^5}} \end{array} \right\}, \tag{55}$$

and $\Gamma_i'^{(s)}$ denotes the 1st-order partial differentiation of $\Gamma_i^{(s)}$, taken with respect to ξ. The similar process of integration by parts can be performed again for the double-integral on the right hand side of Eq. (54), yielding

$$\begin{aligned} &\int_{-1}^{1}\int_{-1}^{1}\frac{\sqrt{\xi^2+\alpha_1\xi+\alpha_0}}{(X_1-X_2)^2}\Gamma_i'^{(s)}d\xi d\eta = \frac{1}{4}\int_{-1}^{1}\Gamma_i'^{(s)} \left[\begin{array}{l} \dfrac{(2\xi+\alpha_1)\sqrt{\xi^2+\alpha_1\xi+\alpha_0}}{(X_1-X_2)^2} \\ -\dfrac{1}{2}\ln\left(2\xi+\alpha_1+2\sqrt{\xi^2+\alpha_1\xi+\alpha_0}\right) \end{array} \right]\Bigg|_{\xi=-1}^{\xi=1} d\eta \\ &-\frac{1}{4}\int_{-1}^{1}\int_{-1}^{1}\frac{\Gamma_i''^{(s)}(2\xi+\alpha_1)\sqrt{\xi^2+\alpha_1\xi+\alpha_0}}{(X_1-X_2)^2}\,d\xi d\eta + \frac{1}{8}\int_{-1}^{1}\int_{-1}^{1}\Gamma_i''^{(s)}\ln\left(2\xi+\alpha_1+2\sqrt{\xi^2+\alpha_1\xi+\alpha_0}\right)d\xi d\eta\,, \end{aligned} \tag{56}$$

where $\Gamma_i''^{(s)}$ represents the 2nd-order partial differentiation of $\Gamma_i^{(s)}$ with respect to ξ. It is noted that the last double-integral on the right hand side of Eq. (56) is weakly singular. For removing its singularity, it can be integrated by parts once again to give

https://doi.org/10.1017/jmech.2012.140 Published online by Cambridge University Press

$$\int_{-1}^{1}\int_{-1}^{1}\Gamma_i''^{(s)}\ln\left(2\xi+\alpha_1+2\sqrt{\xi^2+\alpha_1\xi+\alpha_0}\right)d\xi d\eta$$
$$=\int_{-1}^{1}\Gamma_i''^{(s)}\left[\begin{array}{l}-\sqrt{\xi^2+\alpha_1\xi+\alpha_0}\\+\dfrac{1}{2}(2\xi+\alpha_1)\ln\left(2\xi+\alpha_1+2\sqrt{\xi^2+\alpha_1\xi+\alpha_0}\right)\end{array}\right]\Bigg|_{\xi=-1}^{\xi=1}d\eta \tag{57}$$
$$-\int_{-1}^{1}\int_{-1}^{1}\Gamma_i'''^{(s)}\left[\begin{array}{l}-\sqrt{\xi^2+\alpha_1\xi+\alpha_0}\\+\dfrac{1}{2}(2\xi+\alpha_1)\ln\left(2\xi+\alpha_1+2\sqrt{\xi^2+\alpha_1\xi+\alpha_0}\right)\end{array}\right]d\xi d\eta\ ,$$

where $\Gamma_i'''^{(s)}$ represents the 3rd-order partial differentiation of $\Gamma_i^{(s)}$ with respect to ξ. By substituting Eqs. (54), (56), and (57) into Eq. (49b), one may obtain

$$K_{is}=\int_{-1}^{1}\frac{\Phi_i^{(s)}\big|_{\xi=-1}^{\xi=1}}{(X_1-X_2)^2}d\eta-\frac{1}{2}\int_{-1}^{1}\int_{-1}^{1}\frac{\Psi_i^{(s)}}{(X_1-X_2)^2}\,d\xi d\eta$$
$$+\frac{1}{4}\int_{-1}^{1}\left[\begin{array}{l}-\Gamma_i''^{(s)}\sqrt{\xi^2+\alpha_1\xi+\alpha_0}\\+\ln\left(2\xi+\alpha_1+2\sqrt{\xi^2+\alpha_1\xi+\alpha_0}\right)\left[\dfrac{\Gamma_i''^{(s)}}{2}(2\xi+\alpha_1)-\Gamma_i'^{(s)}\right]\end{array}\right]\Bigg|_{\xi=-1}^{\xi=1}d\eta \tag{58}$$
$$+\frac{1}{4}\int_{-1}^{1}\int_{-1}^{1}\Gamma_i'''^{(s)}\left[\begin{array}{l}\sqrt{\xi^2+\alpha_1\xi+\alpha_0}\\-\dfrac{1}{2}(2\xi+\alpha_1)\ln\left(2\xi+\alpha_1+2\sqrt{\xi^2+\alpha_1\xi+\alpha_0}\right)\end{array}\right]d\xi d\eta\ ,$$

where $\Phi_i^{(s)}$ and $\Psi_i^{(s)}$ are defined by

$$\Phi_i^{(s)}=\frac{-2N^{(s)}J_i(2\xi+\alpha_1)\left(xp_i-\sum_{c=1}^{k}N^{(c)}x_i^{(c)}\right)}{\sqrt{A_4^3}\sqrt{\xi^2+\alpha_1\xi+\alpha_0}\sqrt{(\xi^2+\beta_1\xi+\beta_0)^3}}$$
$$+\sqrt{\xi^2+\alpha_1\xi+\alpha_0}\left[\frac{\Gamma_i'^{(s)}}{2}(2\xi+\alpha_1)-2\Gamma_i^{(s)}\right], \tag{59a}$$

$$\Psi_i^{(s)}=\Gamma_i''^{(s)}(2\xi+\alpha_1)\sqrt{\xi^2+\alpha_1\xi+\alpha_0}\ . \tag{59b}$$

Recall the nearly singular condition for $f(\eta)\equiv(X_1-X_2)^2\approx 0$ when η approaches η_0. Apparently, the first two integrals in Eq. (58) need further treatment to remove the near-singularity and all other integrals are regular. In principal, $(X_1-X_2)^2$ may be expressed as a polynomial form of the Taylor's series, namely

$$(X_1-X_2)^2=\sum_{n=0}^{m}\frac{f^{(n)}(\eta_0)}{n!}(\eta-\eta_0)^n\ . \tag{60}$$

From algebraic arrangement of Eq. (60), one may obtain

$$\frac{1}{(X_1-X_2)^2}=\frac{1}{A_m\prod_{n=1}^{m}(\eta-\lambda_n)}\ , \tag{61}$$

where the symbol "Π" stands for the product of series terms, λ_n are the roots of the polynomial series given in Eq. (60), and A_m is defined by $A_m=f^{(m)}(\eta_0)/m!$. Under the nearly singular condition (*i.e.* $f(\eta)\approx 0$), only a pair of conjugate roots, say λ_1 and λ_2, bear the form as given in Eq. (46), *i.e.*

$$\lambda_{1/2}=\eta_0\pm\Delta i\ , \tag{62}$$

where, again, Δ represents a small value approaching null. Apparently, $\lambda_{1/2}$ may be determined by numerically solving $f(\eta)=0$ and choosing the pair of conjugate roots with near-zero imaginary parts. Alternatively, these roots may also be analytically determined by the Ferrari's solution [19] to the quartic form of its Taylor's series as de-

https://doi.org/10.1017/jmech.2012.140 Published online by Cambridge University Press

scribed in Eq. (47). The authors have extensively performed numerical experiments to test the accuracy of using the quartic solution. The results have shown that the Ferrari's solution may ideally satisfy $f(\lambda_{1/2}) = 0$ with very insignificant error (less than 10^{-12}). In principal, Eq. (61) may be analytically rewritten into

$$\frac{1}{f(\eta)} = \frac{\upsilon_1}{\eta - \lambda_1} + \frac{\upsilon_2}{\eta - \lambda_2} + F(\eta) \ , \tag{63}$$

where $F(\eta)$ is a regular function, being smooth and well-behaved in the vicinity of η_0; the coefficients υ_1 and υ_2 are determined by

$$\upsilon_{1/2} = 1/f'(\lambda_{1/2}) \ . \tag{64}$$

Thus, the regular function $F(\eta)$ is defined by

$$\begin{aligned} F(\eta) &= \frac{1}{f(\eta)} - \frac{\upsilon_1}{\eta - \lambda_1} - \frac{\upsilon_2}{\eta - \lambda_2} \\ &= \frac{(\eta - \lambda_1)(\eta - \lambda_2) - \upsilon_1 f(\eta)(\eta - \lambda_2) - \upsilon_2 f(\eta)(\eta - \lambda_1)}{f(\eta)(\eta - \lambda_1)(\eta - \lambda_2)} \ . \end{aligned} \tag{65}$$

As a direct consequence of applying Eq. (63), one obtains

$$\int_{-1}^{1} \frac{\Phi F_i^{(s)}}{(X_1 - X_2)^2} \, d\eta = \sum_{k=1}^{2} \upsilon_k \int_{-1}^{1} \frac{\Phi F_i^{(s)}}{\eta - \lambda_k} \, d\eta + \int_{-1}^{1} F(\eta) \Phi F_i^{(s)} d\eta \tag{66}$$

in which $\Phi F_i^{(s)}$ is defined by

$$\Phi F_i^{(s)} = \Phi_i^{(s)} \Big|_{\xi=-1}^{\xi=1} \tag{67}$$

and the first two integrals can be integrated by parts twice, resulting in

$$\begin{aligned} &\int_{-1}^{1} \frac{\Phi F_i^{(s)}}{(X_1 - X_2)^2} \, d\eta \\ &= \sum_{k=1}^{2} \upsilon_k \left\{ \begin{array}{l} \Phi F_i^{(s)} \ln(\eta - \lambda_k) - \Phi F_i'^{(s)} (\eta - \lambda_k) \left[\ln(\eta - \lambda_k) - 1 \right] \Big|_{\eta=-1}^{\eta=1} \\ + \int_{-1}^{1} \Phi F_i''^{(s)} (\eta - \lambda_k) \left[\ln(\eta - \lambda_k) - 1 \right] d\eta \end{array} \right\} + \int_{-1}^{1} F(\eta) \Phi F_i^{(s)} d\eta \ , \end{aligned} \tag{68}$$

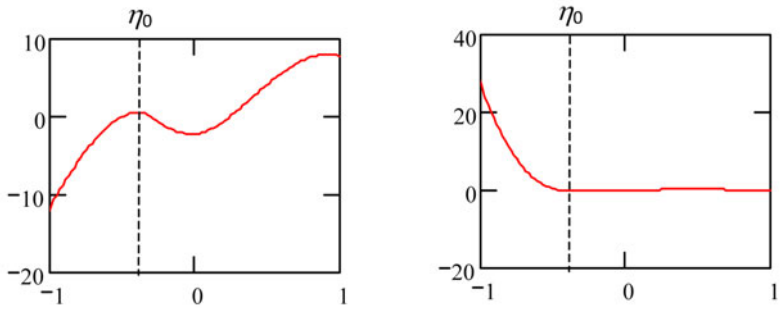
where $\Phi F_i'^{(s)}$ and $\Phi F_i''^{(s)}$ stand for taking differentiation of $\Phi F_i^{(s)}$ with respect to η once and twice, respectively. Apparently, for the nearly singular condition when η approaches λ_k, all integrands in Eq. (68) shall remain smooth and behave regularly and, thus, numerical computation of these integrals will not present any difficulty at all. However, it should be noted that the first integral in Eq. (68), denoted herein by $\Phi_{ki}^{(s)}$, needs to be treated with care. Figures 6(a) and 6(b) show the variations of $\Phi_{1i}^{(s)}$ for its real and imaginary part, respectively. Since the variations of $\Phi_{2i}^{(s)}$ resemble those of $\Phi_{1i}^{(s)}$, they are not shown. As can be seen from Fig. 6(a), due to the fluctuation of the real part in the vicinity of η_0, accurate computation of this integral shall require decomposition of this integral at η_0 such that Eq. (68) is rewritten as

$$\int_{-1}^{1} \frac{\Phi F_i^{(s)}}{(X_1 - X_2)^2} \, d\eta = \sum_{k=1}^{2} \upsilon_k \left\{ \begin{array}{l} \left\langle \Phi F_i^{(s)} \ln(\eta - \lambda_k) - \Phi F_i'^{(s)} (\eta - \lambda_k) \left[\ln(\eta - \lambda_k) - 1 \right] \right\rangle \Big|_{\eta=-1}^{\eta=1} \\ + \int_{-1}^{\eta_0} \Phi_{ki}^{(s)} \, d\eta + \int_{\eta_0}^{1} \Phi_{ki}^{(s)} \, d\eta \end{array} \right\} + \int_{-1}^{1} F(\eta) \Phi F_i^{(s)} d\eta \ . \tag{69}$$

Likewise, the similar process can also be applied to regularize the nearly singular double-integral in Eq. (58). By use of Eq. (63) and the technique of integration by parts, the double-integral can be formulated as

$$\begin{aligned} &\int_{-1}^{1} \int_{-1}^{1} \frac{\Psi_i^{(s)}}{(X_1 - X_2)^2} \, d\xi \, d\eta \\ &= \sum_{k=1}^{2} \upsilon_k \left\{ \begin{array}{l} \int_{-1}^{1} \left\langle \Psi_i^{(s)} \ln(\eta - \lambda_k) - \Psi_i'^{(s)} (\eta - \lambda_k) \left[\ln(\eta - \lambda_k) - 1 \right] \right\rangle \Big|_{\eta=-1}^{\eta=1} d\xi \\ + \int_{-1}^{1} \int_{-1}^{\eta_0} \Psi_{ki}^{(s)} \, d\eta \, d\xi + \int_{-1}^{1} \int_{\eta_0}^{1} \Psi_{ki}^{(s)} \, d\eta \, d\xi \end{array} \right\} + \int_{-1}^{1} \int_{-1}^{1} F(\eta) \Psi_i^{(s)} d\xi d\eta \ , \end{aligned} \tag{70}$$

https://doi.org/10.1017/jmech.2012.140 Published online by Cambridge University Press



(a) Real part (b) Imaginary part

Fig. 6 Fluctuation of Φ_1 for the example case when $\delta = 10^{-5}$: (a) real part; (b) imaginary part

where $\Psi_{ki}^{(s)}$ is defined by

$$\Psi_{ki}^{(s)} = \Psi_i''^{(s)}(\eta - \lambda_k)\left[\ln(\eta - \lambda_k) - 1\right] . \tag{72}$$

For verifying the veracity and testing the accuracy of the regularized forms, the same numerical example as defined in (26) was tested again. Consistently, the 14- point Gauss integration scheme was employed for the calculation. Providing a comparison platform, MathCAD was also used to compute the original integral, given in Eq. (40). For various δ_0 decreasing from10^{-1} to 10^{-7}, Tables 2 ~ 4 list all computed values of K_{is} with percentages of difference in comparison with the MathCAD results. As is clear from the comparisons in Tables 2 ~ 4, numerical integrations of the original integral by the Gauss integration scheme will lead to serious numerical errors when δ_0 falls below 10^{-2} with the distance ratio corresponding to $d/D \approx 0.002$. As expected, when the Gauss integration is performed for the regularized integral, satisfactory numerical results are obtained for all distance orders. It is noted that the regularized results of K_{1s} are relatively greater than those of the other components (K_{2s}, K_{3s}). This is mainly due to their relatively small values in comparison with those of K_{2s} and K_{3s} indeed.

Table 2 Numerical values of K_{1s} for the test case

		$\delta = 10^{-1}$	$\delta = 10^{-2}$	$\delta = 10^{-3}$	$\delta = 10^{-5}$	$\delta = 10^{-7}$
$s = 1$	MathCAD	0.143467	0.412664	0.456555	–0.064386	–0.064395
	Gauss Intg. (original)	0.143467 (0.00%)	0.981179 (137.77%)	1.567846 (245.38%)	0.359796 (658.81%)	0.347529 (639.68%)
	Gauss Intg. (regularized)	0.143461 (0.00%)	0.412643 (0.01%)	0.452492 (0.89%)	–0.067979 (5.58%)	–0.067905 (5.45%)
$s = 2$	MathCAD	–0.829896	–1.627065	–1.737971	–0.429290	–0.429211
	Gauss Intg. (original)	–0.829896 (0.00%)	–3.052810 (87.63%)	–4.546666 (161.61%)	–1.460784 (240.28%)	–1.429681 (233.10%)
	Gauss Intg. (regularized)	–0.829896 (0.00%)	–1.627015 (0.00%)	–1.730025 (0.46%)	–0.422289 (1.63%)	–0.422378 (1.59%)
$s = 3$	MathCAD	0.147354	0.354944	0.393554	0.145092	0.145071
	Gauss Intg. (original)	0.147354 (0.00%)	0.598876 (68.724%)	0.860751 (118.71%)	0.333655 (129.96%)	0.328342 (126.33%)
	Gauss Intg. (regularized)	0.147354 (0.00%)	0.354917 (0.00%)	0.398738 (0.94%)	0.141858 (2.23%)	0.141917 (2.17%)
$s = 4$	MathCAD	–0.421162	–0.707383	–0.729065	1.114226	1.114088
	Gauss Intg. (original)	–0.421162 (0.00%)	–2.801487 (296.035%)	–4.895512 (571.48%)	–0.565296 (150.73%)	–0.521655 (146.82%)
	Gauss Intg. (regularized)	–0.421162 (0.00%)	–0.707397 (0.00%)	–0.729571 (0.07%)	1.113804 (0.04%)	1.113682 (0.04%)
$s = 5$	MathCAD	0.221365	0.461664	0.496211	–0.067035	–0.067030
	Gauss Intg. (original)	0.221373 (0.00%)	1.084891 (135.00%)	1.727858 (248.21%)	0.408181 (708.91%)	0.394880 (689.11%)
	Gauss Intg. (regularized)	0.221365 (0.00%)	0.461652 (0.00%)	0.493940 (0.46%)	–0.069040 (2.99%)	–0.068988 (2.92%)
$s = 6$	MathCAD	–0.299787	–0.578548	–0.620582	0.076090	0.076101
	Gauss Intg. (original)	–0.299793 (0.00%)	–1.328639 (129.651%)	–2.097511 (237.99%)	–0.504826 (763.46%)	–0.048877 (742.27%)
	Gauss Intg. (regularized)	–0.299787 (0.00%)	–0.578521 (0.01%)	–0.616355 (0.68%)	0.079814 (4.89%)	0.079736 (4.78%)
$s = 7$	MathCAD	0.202341	0.411551	0.442589	0.023915	0.023903
	Gauss Intg. (original)	0.202346 (0.00%)	0.863087 (109.72%)	1.330591 (200.64%)	0.366656 (1433.19%)	0.356941 (1393.29%)
	Gauss Intg. (regularized)	0.202341 (0.00%)	0.411535 (0.00%)	0.440525 (0.47%)	0.022103 (7.57%)	0.022137 (7.39%)

https://doi.org/10.1017/jmech.2012.140 Published online by Cambridge University Press

$s = 8$	MathCAD	−0.521527	−0.863575	−0.908566	−0.304121	−0.304071
	Gauss Intg. (original)	−0.521534 (0.00%)	−1.506611 (74.462%)	−2.168946 (138.72%)	−0.781028 (156.82%)	−0.767038 (152.26%)
	Gauss Intg. (regularized)	−0.521527 (0.00%)	−0.863575 (0.00%)	−0.907702 (0.10%)	−0.303401 (0.24%)	−0.303379 (0.23%)

Table 3 Numerical values of K_{2s} for the test case

		$\delta = 10^{-1}$	$\delta = 10^{-2}$	$\delta = 10^{-3}$	$\delta = 10^{-5}$	$\delta = 10^{-7}$
$s = 1$	MathCAD	−0.387012	−14.236564	−323.412124	−292.895607	−287.394815
	Gauss Intg. (original)	−0.387026 (0.00%)	−46.708442 (228.09%)	−732.464278 (126.48%)	−730.355486 (149.36%)	−729.678751 (153.89%)
	Gauss Intg. (regularized)	−0.387012 (0.00%)	−14.236601 (0.00%)	−323.414065 (0.00%)	−292.897271 (0.00%)	−287.396435 (0.00%)
$s = 2$	MathCAD	1.306552	36.641259	811.685891	735.194169	721.406339
	Gauss Intg. (original)	1.306592 (0.00%)	119.119927 (225.10%)	1856.549643 (128.73%)	1851.207587 (151.799%)	1849.493035 (156.373%)
	Gauss Intg. (regularized)	1.306552 (0.00%)	36.641345 (0.00%)	811.689337 (0.00%)	735.196967 (0.00%)	721.409036 (0.00%)
$s = 3$	MathCAD	0.079057	−5.769931	−153.175350	−138.608668	−135.983693
	Gauss Intg. (original)	0.079057 (0.00%)	−19.474939 (237.53%)	−316.292556 (106.49%)	−315.379990 (127.533%)	−315.087063 (131.709%)
	Gauss Intg. (regularized)	0.079057 (0.00%)	−5.769983 (0.00%)	−153.177338 (0.00%)	−138.610331 (0.00%)	−135.985295 (0.00%)
$s = 4$	MathCAD	1.647377	52.006443	1147.248053	1039.195790	1019.714552
	Gauss Intg. (original)	1.647426 (0.00%)	167.619508 (222.305%)	2608.088340 (127.33%)	2600.584353 (150.250%)	2598.176061 (154.794%)
	Gauss Intg. (regularized)	1.647377 (0.00%)	52.006402 (0.00%)	1147.246636 (0.00%)	1039.194601 (0.00%)	1019.713410 (0.00%)
$s = 5$	MathCAD	−0.414599	−15.454694	−349.822563	−316.823449	−310.874782
	Gauss Intg. (original)	−0.414618 (0.01%)	−50.700844 (228.061%)	−794.291174 (127.06%)	−792.005 (149.983%)	−791.270709 (154.530%)
	Gauss Intg. (regularized)	−0.414599 (0.00%)	−15.454736 (0.00%)	−349.823288 (0.00%)	−316.824080 (0.00%)	−310.875391 (0.00%)
$s = 6$	MathCAD	0.506291	19.042508	432.022681	391.263576	383.914520
	Gauss Intg. (original)	0.506301 (0.00%)	61.231007 (221.549%)	958.048460 (121.76%)	955.291756 (144.157%)	954.406761 (150.359%)
	Gauss Intg. (regularized)	0.506291 (0.00%)	19.042555 (0.00%)	432.024499 (0.00%)	391.262102 (0.00%)	383.915939 (0.00%)
$s = 7$	MathCAD	−0.322646	−11.442063	−259.655263	−235.155809	−230.739635
	Gauss Intg. (original)	−0.322655 (0.00%)	−37.042221 (223.737%)	−579.882784 (123.33%)	−578.213858 (145.885%)	−577.678167 (150.36%)
	Gauss Intg. (regularized)	−0.322646 (0.00%)	−11.442089 (0.000%)	−259.656295 (0.00%)	−235.156645 (0.00%)	−230.740440 (0.00%)
$s = 8$	MathCAD	0.477509	16.679570	374.037319	338.766810	332.409313
	Gauss Intg. (original)	0.477524 (0.00%)	53.484195 (220.66%)	834.227234 (123.33%)	831.827882 (145.55%)	831.057447 (150.010%)
	Gauss Intg. (regularized)	0.477509 (0.00%)	16.679600 (0.00%)	374.038328 (0.00%)	338.767651 (0.00%)	332.410124 (0.00%)

Table 4 Numerical values of K_{3s} for the test case

		$\delta = 10^{-1}$	$\delta = 10^{-2}$	$\delta = 10^{-3}$	$\delta = 10^{-5}$	$\delta = 10^{-7}$
$s = 1$	MathCAD	0.646669	11.273999	241.666998	217.259515	213.161358
	Gauss Intg. (original)	0.646678 (0.00%)	36.716115 (225.67%)	539.979585 (123.44%)	534.545354 (146.04%)	534.100348 (150.52%)
	Gauss Intg. (regularized)	0.646669 (0.00%)	11.274048 (0.00%)	241.673477 (0.00%)	217.265230 (0.00%)	213.166910 (0.00%)
$s = 2$	MathCAD	−1.742535	−28.439152	−605.925121	−544.743252	−534.471103
	Gauss Intg. (original)	−1.742575 (0.00%)	−93.103104 (227.38%)	−1368.142946 (125.79%)	−1354.373166 (148.63%)	−1353.020207 (153.15%)
	Gauss Intg. (regularized)	−1.742535 (0.00%)	−28.439262 (0.00%)	−605.938026 (0.00%)	−544.754504 (0.00%)	−534.482072 (0.00%)
$s = 3$	MathCAD	0.169053	4.824014	114.704923	103.056082	101.100422
	Gauss Intg. (original)	0.169038 (0.00%)	15.521370 (221.75%)	233.354028 (103.44%)	231.002107 (124.15%)	230.770963 (128.26%)
	Gauss Intg. (regularized)	0.169053 (0.00%)	4.824073 (0.00%)	114.711229 (0.01%)	103.061601 (0.01%)	101.100422 (0.01%)
$s = 4$	MathCAD	−2.638683	−41.623856	−857.811389	−771.382490	−756.868500
	Gauss Intg. (original)	−2.638701 (0.00%)	−132.154216 (217.50%)	−1923.149348 (124.19%)	−1903.806915 (146.81%)	−1901.906512 (151.29%)

https://doi.org/10.1017/jmech.2012.140 Published online by Cambridge University Press

	Gauss Intg. (regularized)	–2.638683 (0.00%)	–41.623838 (0.00%)	–857.810610 (0.00%)	–771.381836 (0.00%)	–756.867875 (0.00%)
$s = 5$	MathCAD	0.614168	12.182801	261.356141	234.963129	230.531270
	Gauss Intg. (original)	0.614180 (0.00%)	39.794927 (226.65%)	585.505279 (124.03%)	579.612993 (146.68%)	579.033958 (151.17%)
	Gauss Intg. (regularized)	0.614168 (0.00%)	12.182828 (0.00%)	261.359612 (0.00%)	234.966202 (0.00%)	230.534267 (0.00%)
$s = 6$	MathCAD	–1.071223	–15.284097	–323.029366	–290.425120	–284.950987
	Gauss Intg. (original)	–1.071218 (0.00%)	–48.303992 (216.04%)	–706.432974 (118.69%)	–699.323542 (140.79%)	–698.625164 (145.174%)
	Gauss Intg. (regularized)	–1.071223 (0.00%)	–15.284156 (0.00%)	–323.036226 (0.00%)	–290.431010 (0.00%)	–284.956816 (0.00%)
$s = 7$	MathCAD	0.559687	9.093824	194.058928	174.462993	171.172851
	Gauss Intg. (original)	0.559689 (0.00%)	29.139086 (220.427%)	427.510492 (120.30%)	423.207882 (142.58%)	422.785162 (146.99%)
	Gauss Intg. (regularized)	0.559687 (0.00%)	9.093857 (0.00%)	194.062330 (0.00%)	174.465946 (0.00%)	171.175728 (0.00%)
$s = 8$	MathCAD	–0.843084	–13.070865	–279.336625	–251.122778	–246.386292
	Gauss Intg. (original)	–0.843090 (0.00%)	–41.893883 (220.51%)	–614.827284 (120.10%)	–608.637316 (142.37%)	–608.029329 (146.78%)
	Gauss Intg. (regularized)	–0.843084 (0.00%)	–13.070892 (0.00%)	–279.337777 (0.00%)	–251.123736 (0.00%)	–246.387214 (0.00%)

5. CONCLUSIVE REMARKS

In the conventional BEM analysis for heat conduction in thin media, the so called "nearly singular" integration by the usual numerical scheme will yield invalid numerical values. For 3D analysis, the integrals in the associated boundary integral equation reveal themselves with the traits of strong singularity and hyper-singularity. As reported in the past literature, resolutions to this numerical difficulty usually involve intricate mathematical techniques to yield proper integration values. As a direct consequence, these proposed techniques are not so friendly for implementation in programming. For 2D problems, this problem may be easily resolved by the scheme of integration by parts; however, this technique has not been applied to 3D problems yet. This paper presents very explicit formulations of the regularized integrals to treat the 3D potential problems by the BEM. For verification of their veracities, a numerical example considering an integration element of a partial spherical surface was investigated. Numerical results show that numerical integrations of the regularized integrals by the conventional Gauss Quadrature rule can properly yield accurate values, no matter how small the distance ratio is. As the major contribution, the present work suggests that the technique of integration by parts can be applied for regularizing the strongly singular and hyper-singular integrals in other 3D cases of engineering problems- the 3D BEM analysis in elastostatics for example.

ACKNOWLEDGMENTS

The authors gratefully acknowledge the financial support of the National Science Council of Taiwan, Republic of China (Grant Number: NSC 96-2221-E-035-011-MY3).

REFERENCES

1. Kayhani, M. H., Norouzi, M. and Amiri Delouei, A., "A General Analytical Solution for Heat Conduction in Cylindrical Multilayer Composite Laminates," *International Journal of Thermal Sciences*, **52**, pp. 73-82 (2012).
2. Haji-Sheikh, A., Amos, Donald E., and Beck, J. V., "Axial Heat Conduction in a Moving Semi-Infinite Fluid," *International Journal of Heat and Mass Transfer*, **51**, pp. 4651–4658 (2008).
3. Ma, C.-C. and Chang, S.-W., "Analytical Exact Solutions of Heat Conduction Problems for Anisotropic Multi-Layered Media," *International Journal of Heat and Mass Transfer*, **47**, pp. 1643–1655 (2004).
4. Rizzo, F. J., "An Integral Equation Approach to Boundary Values Problems of Classical Elastostatics," *Quarterly of Applied Mathematics*, **40**, pp. 83-95 (1967).
5. Lauricella, G., *Sur Pintégration De Péquation Relative Á Pequilibre Des Plaques Élastiques Encastrées*, Acta Math., 32 (in French).
6. Massonnet, C. E., *Numerical Use of Integral Procedures, Stress Analysis*, O.C. Zienkiewicz and Z.S. Holister, eds., John Wily and Sons, London, U.K. (1965).
7. Kupradze, V. D., *Potential Methods in the Theory of Elasticity. Translated From Russian by Israel Program for Scientific Translation*, Jerusalem, Israel., (1963).
8. Hong, H.-K. and Chen, J.-T., "Derivations of Integral Equations of Elasticity," *Journal of Engineering Mechanics*, ASCE, **114**, pp. 1028–1044 (1988).
9. Zozulya, V. V., "Divergent Integrals in Elastostatics: Regularization in 3-D Case," *CMES: Computer Modeling in Engineering & Sciences*, **70**, pp. 253–349 (2010).
10. Chen, J. T. and Hong, H-K., "Review of Dual Boundary Element Methods with Emphasis on Hypersingular Integrals and Divergent Series," *Applied Mechanics Reviews*, **52**, pp. 17–33 (1999).

https://doi.org/10.1017/jmech.2012.140 Published online by Cambridge University Press

11. Guz, A. N. and Zozulya, V. V., "Fracture Dynamics with Allowance for a Crack Edges Contact Interaction," *International Journal of Nonlinear Sciences and Numerical Simulation*, **2**, pp. 173–233 (2001).
12. Tanaka, M., Sladek, V. and Sladek, J., "Regularization Techniques Applied to Boundary Element Methods," *Applied Mechanics Reviews*, **47**, pp. 457–499 (1994).
13. Granados, J. J. and Gallego, R., "Regularization of Nearly Hypersingular Integrals in the Boundary Element Method," *Engineering Analysis with Boundary Elements*, **25**, pp. 165–184 (2001).
14. Tomioka, S. and Nishiyama, S., "Analytical Regularization of Hypersingular Integral for Helmholtz Equation in Boundary Element Method," *Engineering Analysis with Boundary Elements*, **34**, pp. 393–404 (2010).
15. de Lacerda, L. A. and Wrobel, L. C., "Hypersingular Boundary Integral Equation for Axisymmetric Elasticity," *International Journal for Numerical Methods in Engineering*, **52**, pp. 1337–1354 (2001).
16. Shiah, Y. C. and Shi, Y.-X., "Heat Conduction Across Thermal Barrier Coatings of Anisotropic Substrates," *International Communications in Heat and Mass Transfer*, **33**, pp. 827–835 (2006).
17. Shiah, Y. C., Chen, Y. H. and Kuo, W. S., "Analysis for the Interlaminar Stresses of Thin Layered Composites Subjected to Thermal Loads," *Composites Science and Technology*, **67**, pp. 2485–2492 (2007).
18. Chen, J. T., Kuo, S. R., Chen, W. C. and Liu, L. W., "On the Free Terms of the Dual BEM for the Two and Three-Dimensional Laplace Problems," *Journal of Marine Science and Technology*, **8**, pp. 8–15 (2000).
19. Brookfield, G., "Factoring Quartic Polynomials: A Lost Art," *Mathematics Magazine*, **80**, pp. 67–70 (2007).
20. http://en.wikipedia.org/wiki/Quartic_function.

(Manuscript received July 23, 2012,
accepted for publication August 31, 2012.)

https://doi.org/10.1017/jmech.2012.140 Published online by Cambridge University Press